Energy Reports 7 (2021) 7090–7105

Contents lists available at ScienceDirect

Energy Reports

journal homepage: www.elsevier.com/locate/egyr

Research paper

Life cycle assessment of compressed air, vanadium redox flow battery, and molten salt systems for renewable energy storage

Manal AlShafi *, Yusuf Bicer

Division of Sustainable Development, College of Science and Engineering, Hamad Bin Khalifa University, Qatar Foundation, Doha, Qatar

ARTICLE INFO

Article history:
Received 10 May 2021
Received in revised form 21 September 2021
Accepted 29 September 2021
Available online 26 October 2021

Keywords:
Emissions
Environment
Impact assessment
Renewable energy
Solar energy

ABSTRACT

Energy storage systems critically assist in the implementation of renewable energy sources. However, greenhouse gas emissions associated with the energy storage methods have received insufficient attention, especially for arid climate implementation. This paper considers three energy storage techniques that can be suitable for hot arid climates namely; compressed air energy storage, vanadium redox flow battery, and molten salt thermal storage and performs a comprehensive life cycle assessment analysis to comparatively evaluate the environmental impacts per kWh of energy. The results show that, when solar photovoltaic electricity is stored, the redox-flow battery has the highest global warming potential, corresponding to 0.121 kg CO_2 eq./kWh, whereas the molten salt has the least with a value of 0.0306 kg CO_2 eq./kWh. In contrast, the lowest ozone layer depletion is observed for the compressed air storage unit with a value of 7.24×10^{-13} kg R11 eq./kWh. In sensitivity analysis, it is found that using solar photovoltaic electricity for the considered energy storage methods rather than grid electricity critically reduces the associated environmental impacts, emphasizing the importance of implementing more renewables in the grid mix. The global warming potentials of compressed air and vanadium redox flow battery decrease by 0.599 and 0.420 kg CO_2 eq./kWh, respectively in case photovoltaic electricity is stored instead of grid electricity. It is also found that the production stage of the storage systems accounts for the highest share of carbon footprint.

1. Introduction

Renewable energy sources are sporadic and have challenges in providing stable electricity to our communities. Although they are intermittent, this intermittency can be overcome by using proper energy storage methods to enable a more regular electricity supply. To synchronize energy production and utilization, the implementation of energy storage systems (ESS) is necessary. ESSs vary in numerous aspects, such as environmental impact, efficiency, and cost. Such parameters shall be evaluated comprehensively for all storage systems to reach a decision in terms of feasibility. Among several criteria, environmental concerns are critical, especially considering the intensive climate change consequences faced worldwide. Life cycle assessment (LCA) is a decent* technique for assessing the environmental impacts, weighing the benefits against their drawbacks, and assisting the decision-makers in implementing the most suitable storage technique (Alqub, 2017). A LCA study provides information to assist in looking for possible solutions to environmental concerns related to product life cycles. It was first implemented to compare alternatives of defined end products, e.g., milk packaging forms. However, it has been incorporated into higher strategic levels, covering policy making and decisions at a corporate level (Goedkoop, 2013). The practitioner selects a life cycle impact assessment (LCIA) technique and other essential means in life cycle assessment software during LCA analysis. LCIA is the life cycle assessment stage that assesses the magnitude of all elementary flows' contribution to an environmental impact. The purpose is to examine the assessed product/system from an environmental perspective using category indicators and impact categories synchronous with inventory analysis results (Oró et al., 2012; Lacy et al., 2015).

Numerous LCA studies were performed for many different energy storage systems. A study (Oró et al., 2012) was conducted for three different thermal energy storage systems for solar power plants to compare their environmental impacts using Eco-indicator 99 method. The systems studied were (i) sensible heat storage in liquid (molten salts) thermal storage media, (ii) solid high-temperature concrete, and (iii) storage of latent heat utilizing phase-changing material. During the manufacturing phase, the two systems, which use molten salts as storage material, were similar in their impact results. Besides, solid media-based storage has shown the most negligible environmental impact per kWh stored energy compared to others due to the system's simplicity (Oró et al., 2012). An estimation was

* Corresponding author.
E-mail addresses: malshafi@hbku.edu.qa (M. AlShafi), ybicer@hbku.edu.qa (Y. Bicer).

https://doi.org/10.1016/j.egyr.2021.09.161

made for greenhouse gas (GHG) emissions and global warming potential (GWP) from the hypothetical carbon capture, utilization, and storage (CCUS) case in a natural gas combined cycle power plant (NGCC) by utilizing the LCA methodology (Lacy et al., 2015). Supercritical pulverized carbon (SCPC), NGCC with no carbon capture, geothermal, wind, nuclear, and mini-hydro were compared with other electricity-generation technologies. The NGCC power plant with CCUS produced 0.177 kg CO_2 eq./kWh. It represents 21% and 36% of the estimated NGCC (without CCUS) and SCPC values, respectively; therefore, it has 24% less GHG emissions than the geothermal case (Lacy et al., 2015).

There is also a combination of environmental analysis and thermodynamic analysis in the literature. Esfandi et al. (2020) have proposed a hybrid novel system to produce cooling, syngas, and electricity. The study discussed economic, energy, exergy, exergoenvironmental analyses of the combined proposed hybrid system to assess its viability, environmental impact, and performance when implemented in Tehran. It was indicated how the pattern of the production of each useful product relies on the collection of available renewable energies patterns. Another study (Dibazar et al., 2020) has conducted advanced exergy comparison analysis for three organic Rankine cycles (ORC): (i) ORC with single regeneration, (ii) ORC with double regeneration, and (iii) basic ORC. In comparison with the basic ORC, it was shown that the regenerative ORC has a high potential for minimizing irreversibilities. Overall exergy destruction rates of 5.25 kW (45%) and 4.13 (47%) occur for single regeneration ORC and double regeneration ORC, respectively. Ahmadi et al. (2017) evaluated the solar thermal energy use for repowering parallel feed water heating of the power plant unit of Isfahan Mohammed Montazeri. The net exergy and energy efficiencies reached 36.85 and 35.21%, and that is when all high-pressure feedwater heaters were replaced with solar collectors. Dabiri et al. (2018) analyzed heat loss and heat transfer in a trapezoidal cavity of a linear Fresnel reflector. It was indicated that increasing the cavity angle increases the total value of the heat transfer rate.

Recent literature has developed a model to determine the life cycle GHG emissions, and the net energy ratios for the energy storage systems of (i) pumped hydroelectric energy storage, (ii) adiabatic, and (iii) conventional compressed air energy storage (CAES). The GHG emissions of these three different energy storage methods were found to be (i) 211.1, (ii) 231.2, and (iii) 368.2 g CO_2 eq./kWh, respectively. An evaluation was done for the GHG emissions associated with the life cycle stages of construction, operation, and decommissioning of energy storage systems (ESSs). The emissions were at the highest in the operational phase of all ESSs (Kapila et al., 2019). Raugei et al. (2020) conducted a LCA for a 100 MW ground-mounted photovoltaic system with 60 MW of lithium manganese oxide battery under a set of storage scenarios and irradiation ranges. It was indicated that the GWP and energy payback time increased by 7 and 30%, respectively, compared to the case of photovoltaics (PV) with no storage. The sustainability of lithium-ion, lead–acid compressed air, pumped hydro energy storage, and flow batteries concentration gradient were investigated by implementing a multi-dimensional LCA. The analysis concluded that the lead–acid battery resulted in the most severe damage to ecosystem diversity and human health. In contrast, the CAES is the highest in resource availability, and the lead–acid battery is a non-preferable system for the global warming potential (Stougie et al., 2018). For a cloakroom and club building in Zurich, a LCA of PV-battery system was implemented. The installation of PV-battery storage indicated 10%–17% of GHG emissions reduction compared to the average value of Swiss electricity supply (Stolz et al., 2019). A study by (Zhang et al., 2017) identified the life cycle of a 20 MW scale cryo-battery system. A comparison was done with natural gas turbine generators and equivalent diesel-electric generators alternatives to define a cryo-battery system's net GHG emissions savings potential. The GHG emissions of the electricity grid were in the range of 30–232 kg CO_2 eq./MWh (Zhang et al., 2017). Vandepaer et al. (2017) have evaluated the environmental performance of Lithium Metal Polymer batteries stationary using the LCA methodology compared to the Li-ion units. The polytetrafluoroethylene production, utilized only in Li-ion batteries, was the major contributor to the category of ozone layer depletion and was also a significant source of global warming emissions.

A storage device, ColdPeak, was recently studied in the literature, as it demonstrated distinctive properties for charging and discharging of power (De Falco et al., 2017). The unit was recently analyzed from an environmental perspective using the LCA method. A conventional system was compared with the air conditioning system integrated with ColdPeak from an environmental viewpoint. It has estimated the same cold energy potentiality and involving a sensitivity analysis on the innovative device's energy-saving potential. A major reduction of environmental footprint related to GWP (−17%), eutrophication potential (−18%), acidification potential (−15.5%), human health (−18%), eco-toxicity (−16%), and fossil depletion (−18%) was shown in the integration of the cold unit storage (De Falco et al., 2017). A new Power-to-Gas approach for energy storage from volatile renewable sources was also studied to store methane and hydrogen in geological formations (Tschiggerl et al., 2018). In the demonstration project, the LCA approach constructed and tested alternative business models for their environmental impacts. Their analysis indicated that the energy source is vital for the Power-to-Gas plant's environmental performance, regardless of the implemented business model (Tschiggerl et al., 2018). Peng et al. (2013) have examined the environmental and sustainability performance of PV-based electricity generation through conducting a comprehensive review of LCA studies of well-known PV systems: Multi-crystalline (multi-Si), mono-crystalline (mono-Si), copper indium selenium (CIS thin-film), *Cadmium telluride* (CdTe thin film), amorphous silicon (a-Si), and several advanced techniques of PV. The mono-Si systems of PV have revealed the worst environmental performance as high energy intensity is used up during solar cell production. The total energy input of thin-film PV systems (CdTe, CIS, and a-Si) was between 710–1990 MJ/m^2. As a result, the energy payback time and GHG emission rates were in the range of 0.75 to 3.5 years and 10.5 to 50 g CO_2 eq./kWh, respectively. A study for biogas using on-site data was conducted and found that GWP was in the range of 3.8–12.5 g of CO_2 eq. in biogas (Rehl et al., 2012). A case study in the UK was done to compare anaerobic digestion's environmental impact with energy and organic fertilizers' production against alternative approaches: Landfill with electricity production and incineration with energy production by combined heat power. The incineration option was better for environmental impact for nutrient enrichment and photochemical ozone (Evangelisti et al., 2014).

Referring to the Sustainable Development Goals (SDG), this research has been motivated and initiated to address SDG 7 (affordable and clean energy) and SDG 13 (climate action). It addresses the gap between renewable sources and energy storage implementation due to the intermittent nature of renewables. Hence, an environmental impact assessment is conducted to address SDG 13 and promote renewables under SDG 7. The study compares the environmental emissions of storing 1 kWh of energy for three different energy storage systems: Compressed air energy storage, vanadium redox flow batteries, and molten salt thermal storage. The study is conducted using the GaBi software and the CML 2001 (2016) LCIA method. The novelty of this study lies under these points: (i) There is a need for more environmentally friendly energy storage methods to complete the

environmental friendliness of renewable energy sources. Therefore, several energy storage methods must be compared in terms of their environmental impacts. (ii) This study initially considers the storage phase of energy and production of energy from selected renewable energy to represent the complete life cycle of the energy production to discharge. (iii) This work considers more suitable energy storage techniques for hot arid climates by building the research upon our previous studies (AlShafi and Bicer, 2021, 2020) to select the most feasible energy storage methods considering several hot arid climate criteria, including water use, efficiency, thermal degradation, etc. Overall, this study presents a comparative evaluation of three different energy storage methods by conducting a comprehensive life cycle assessment analysis. The main objectives of this work are (i) to perform a life cycle assessment study for different types of energy storage systems, (ii) to evaluate the environmental impacts of each system, (iii) to conduct sensitivity analysis on the significant hot spot parameters, (iv) to identify the most sustainable and environmentally friendly storage technique for implementation.

2. Methodology

LCA is a tool based on a systematic examination of activities or products' environmental effects, revealing environmental dimensions of sustainability. It consists of four main phases: Goal and scope definition, life cycle inventory, impact assessment, and interpretation, following the ISO 14044:2006 standards (Goedkoop, 2013). The goal and scope phase requires a careful explanation for the product and system boundaries description. Life cycle inventory is where overall environmental outputs and inputs concerning a product or service, e.g., energy use, raw materials, waste streams, and pollutants' emissions, are collected (Goedkoop, 2013). LCIA classifies and evaluates the environmental impacts and translating these impacts into environmental themes such as human health or global warming. Last comes the interpretation step, where it is checked whether the results and conclusions are well-substantiated and requiring multiple tests to prove that the procedure and data appropriately support the decisions used (Goedkoop, 2013; Peng et al., 2013). In this work, GaBi software is utilized for the analysis, which provides a constantly updated and easily accessible database of a system or a product (Rehl et al., 2012). Furthermore, it considers the effect on the environment providing alternative options for distribution, manufacturing, pollution, sustainability, etc. It assists businesses to reach out to the finest possible product sustainability performance by utilizing life cycle assessments (LCA) with the most updated and accurate databases.

2.1. Goal and scope

The goals of this LCA study can be summarized as follows:

- Performing a life cycle analysis for comparing the environmental impacts of different energy storage systems for a better understanding and implementation in hot arid climates.
- Assisting decision-makers in deciding on the implementation of energy storage methods considering the life cycle emissions.
- Assessment of hotspots in the selected energy storage methods in terms of environmental impacts.
- Conducting a sensitivity analysis to understand the effects of changing the main processes intensively contributing to environmental impacts.

The selected methods represent each main energy storage category (e.g., thermal-molten salt, mechanical-compressed air, electrochemical-VRF-B) applied to hot arid climates. The boundary of this LCA study comprehends stages from the system manufacturing and their use, as shown in Fig. 1. The feed-in of energy represents the system's energy input, whether it is electricity, thermal or mechanical energy for the considered systems. In contrast, the feed out of energy represents the electrical energy produced/discharged from the system. The functional unit is selected to be a 1-kilowatt hour (kWh) of energy.

The manufacturing stage includes the material required for building the ESS infrastructure; the use phase has the constructed system and electricity as an input. This study has excluded the disposal, recycling, and maintenance stages, as sufficient data were not found for several systems. The LCIA method implemented in this study is CML 2001 (2016). It is a worldwide applicable impact assessment method that is not restricted to specific regions.

2.2. Expected audience

This study assists stakeholders, scientific researchers, environment quality authority, and municipalities make crucial energy storage deployment decisions, especially for solar energy applications.

2.3. Systems' applications

There are several energy storages companies worldwide focusing on different storage technologies. Siemens AG, Huntorf, and Apex plants are focusing on compressed air energy storage, where they implemented a real physical plant in Germany. VRB Energy is focusing on VRFBs where there is an existing market for the sales of these batteries. Moreover, there are many physical solar thermal molten salt storage plants in the U.S. and Spain, such as SolanaGeneratingStation and AndasolSolarPowerStations.

2.4. Life cycle inventories

The inventory analysis identifies all inputs and outputs of the processes; they can be material, product, or energy flows. Therefore, limitation in accessing or collecting primary data is a concern. The production phase includes the inputs of energy and materials bearing all upstream processes. Every system has an associated inventory table in which quantities of material and energy are expressed. The inventories of this study are collected from the literature studies. The expected lifetime and capacity factors were considered in the LCA. The tables for the inputs and outputs of the relevant flows are set up with the GaBi software (version 6.0) (GaBi, 2021). The systems' lifetime is taken to be 20 years for the VRF-B and CAES. The life cycle inventory used is sourced from Mostert et al. (2018) for compressed air and battery systems. The compressor and motor data for the compressed air were taken from Kapila (2018), whereas the study (Adeoye et al., 2014) is used for the molten salt thermal storage inventory data. The system lifetime for the molten salt unit is taken as 30 years. The energy efficiencies of 53.6% and 77% are considered for CAES and VRF-B, respectively, in the use phase energy input calculations. The calculated overall(solar-to-power) efficiency of 21.8% is used for molten salt storage, where the energy input originates from solar thermal energy (not electricity). In supporting information, Tables S1–S11 show the inventory data used for the three systems. The system boundaries and flowcharts of the three systems are shown in Figs. 2, 3, and 4.

In Fig. 2, the manufacturing of the CAES system infrastructure requires several materials, naphtha as energy input and an internal container. The steel plate and softwood plywood are the

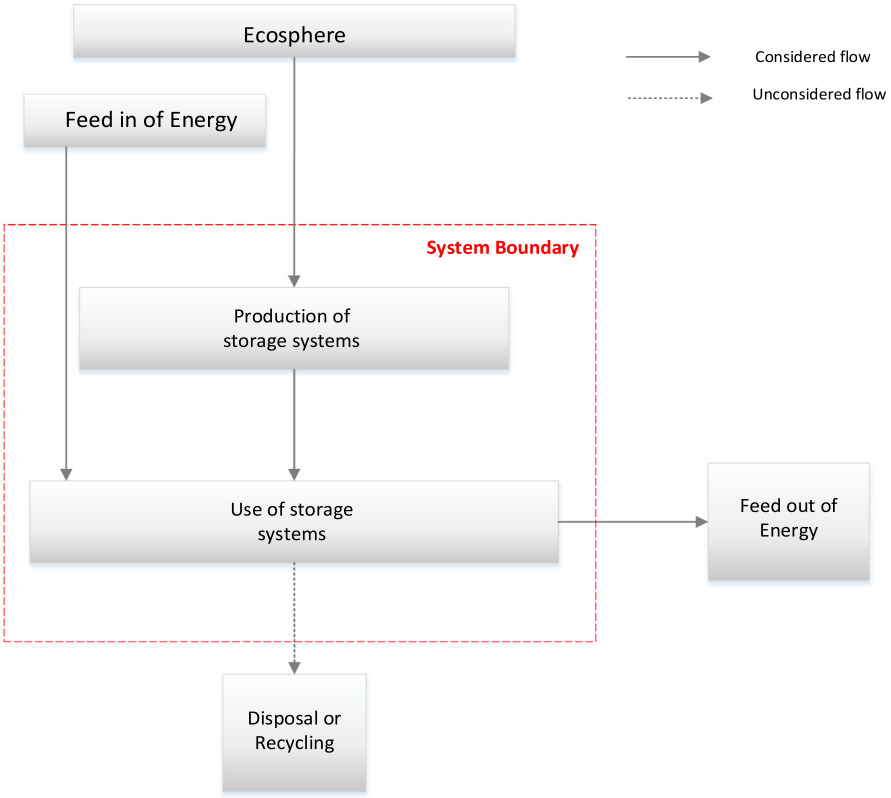

Fig. 1. Energy storage systems life cycle boundary.

only inputs for the container. Containers of a 40' high cube are required during the transportation of the CAES system. Energy input is required to operate/use the storage system. Compared to the literature (Mostert et al., 2018), the system boundaries for both CAES and VRF-B are similar, except for the functional unit. This study is for 1 kWh of storing energy, whereas the literature value as reported in Ref. Mostert et al. (2018) are for 2 MWh of stored energy. Evangelisti et al. (2014) data were collected from several publications, as only several pilot projects were implemented so far. The compressor and motor data (Kapila et al., 2019) were based on actual plant data for the CAES system. In Fig. 3, the VRF-B boundary was set similarly. Here, a 20' high cube container is used. Compared to the literature, the energy flow of the use phase for CAES and VRF-B was only specified as electricity of high voltage; however, for this analysis, electricity from PV was considered. For the molten salt system, only two main processes are essential for the system construction: The solar field construction and molten salt storage, as shown in Fig. 4. Compared to the literature (Adeoye et al., 2014), the maintenance phase was excluded, and that is to match the available/obtained stages of the other two systems for fair system comparison. The data for the molten salt system is based on the Shams-1 CSP plant in UAE. The functional unit from the literature was 800 MWh energy for molten salt.

2.5. Assumptions

Some materials have been substituted compared to the data obtained from Alqub (2017), Evangelisti et al. (2014), AlShafi and Bicer (2021) due to the lack of data in the GaBi (version 6.0) software, which is one of the main limitations. CAES's compressor and motor data were taken from Kapila (2018) because the literature (Evangelisti et al., 2014) provided as a single device. It did not exist in the software; therefore, it was necessary to rely on a different source for these two devices' data. The disposal and maintenance phases were not included as the CAES system (underwater) is newly adopted, and the data for these two phases were not provided in the literature. Further assumptions are detailed below:

Vanadium Redox Flow Battery

- The sulfuric trioxide process instead of sulfuric acid is used as it is made as a precursor to sulfuric acid on an industrial scale and is utilized in sulfuric acid production.
- Metal is used as Vanadium, which is a metallic element.
- Ultrapure water was not available; therefore, a groundwater source was utilized instead.

Compressed Air Storage

- The motor-generator and compressor input was taken from Kapila (2018), as the two processes for Mostert et al. (2018) were unavailable, e.g., the electric motor and air compressor.
- Steel tinplate is used as an alternative for cast iron.
- Polyethylene HDPE is used instead of Nylon as both materials are polymers. In comparison, polyethylene HDPE typically lasts long outdoors.
- Stainless steel replaces chromium steel for the CAES manufacturing stage as stainless steel is more durable than chrome and is more resistant to corrosion.
- Silicone is used instead of rubber for compressor construction. Silicone is a good alternative for rubber as it is greatly heat-resistant, has low levels of toxicity, and rubber-like texture.

Molten Salt Energy Storage

For the solar field construction:

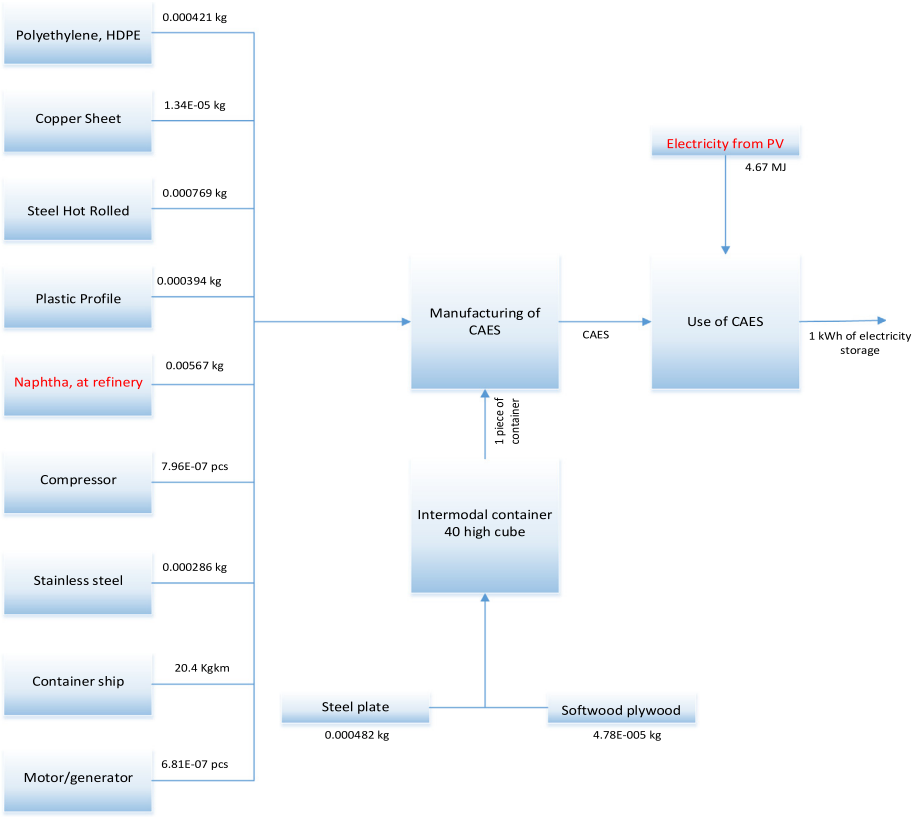

Fig. 2. LCA system boundary and flowchart of the CAES system.

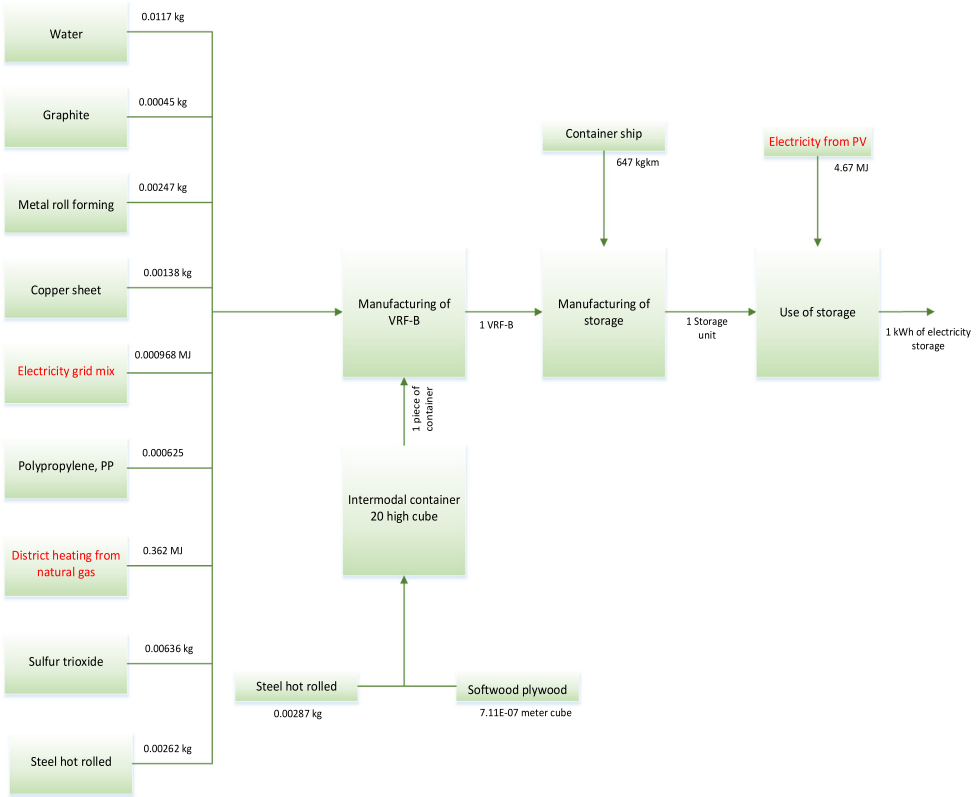

Fig. 3. LCA system boundary and flowchart of VRF-B energy storage system.

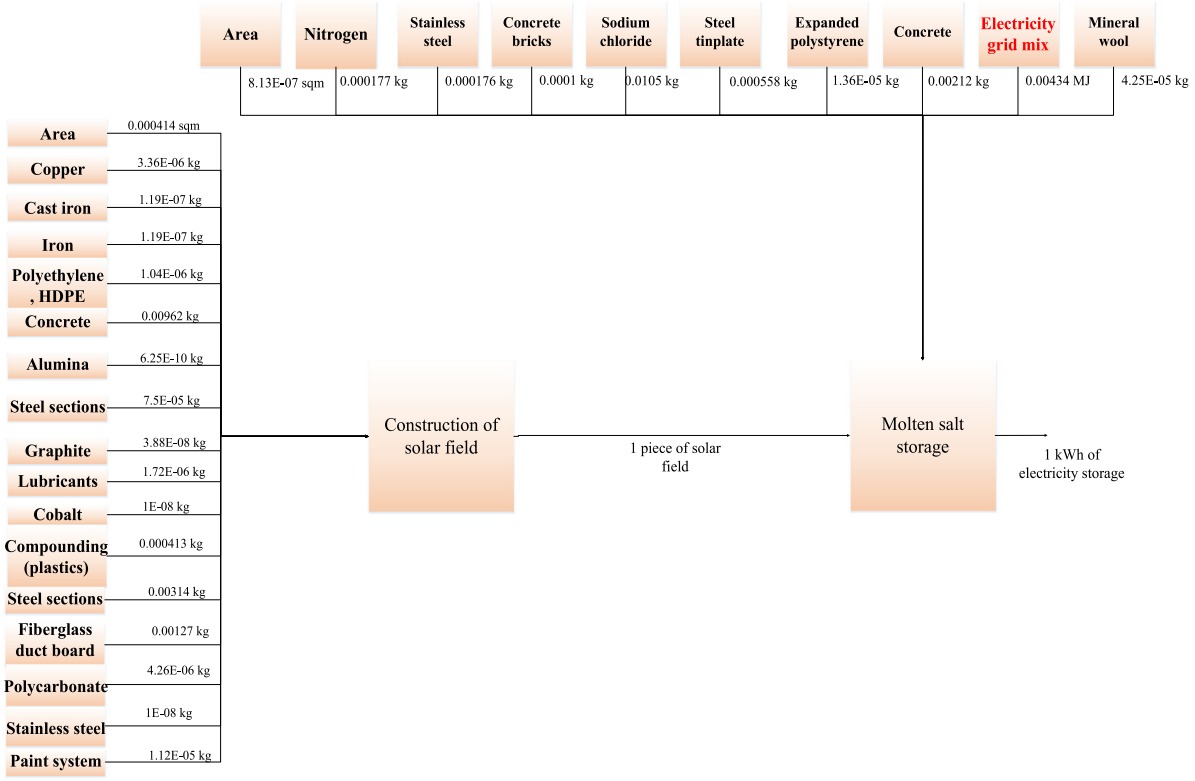

Fig. 4. LCA system boundary and flowchart of the molten salt energy storage system.

- Polycarbonate granulate is utilized instead of the glass container. It is a hard and strong material.
- The duct board replaces the use of laminated glass. It is also an insulation material that is semi-rigid fiberglass frequently utilized in either light commercial or residential heating or cooling.
- Cobalt is utilized instead of Nickel.
- Stainless steel replaces chromium steel. Compared to chrome, stainless steel is more durable and resistant to corrosion.

For the molten salt storage construction:

- Sodium chloride is used as molten salt.
- Concrete bricks replace the refractory ones. Extensive manufacturing labor is not required for the concrete, and the raw form is comparatively inexpensive.
- The expanded polystyrene (EPS) is used as storage insulation instead of glass foam. It is an efficient, light-weighted, and cost-effective material.
- Diesel and electrical energy were summed as one source of energy. This diesel is considered energy input during the manufacturing phase only and is not directly related to grid mix. Diesel is used in heavy vehicles and as a back-up power generator on-site to provide electricity during construction.

2.6. Life cycle impact assessment

There are numerous LCIA procedures established to categorize the environmental impacts associated with the systems. The method utilized for this study is the CML 2001 (2016). It is an impact assessment method initiated by a group of scientists under the principal of the Center of Environmental Science of Leiden University (CML). The selected impact categories for this study are global warming, abiotic depletion, acidification, ozone layer depletion, human toxicity, and marine aquatic ecotoxicity.

2.6.1. Global warming potential (GWP)

It is an index to measure the global warming contribution of a substance released into the atmosphere. It is mainly affected by GHGs emissions, e.g., methane and carbon dioxide. It is expressed for a time horizon of 100 years in kg CO_2 equivalent per kilograms of emission. The burning of different fuels for material production causes global warming; therefore, this impact category is crucial to include in any relevant study.

2.6.2. Ozone layer depletion potential (ODP)

The gradual thinning of the earth's ozone layer in the upper atmosphere is due to the chemical compounds released with chlorine or gaseous bromine coming from several human activities or industries. The unit is specified in kg CFC-11 equivalent per kilograms of emission. Some materials used in storage system production could release harmful gases, e.g., carbon monoxide emitted from steel production.

2.6.3. Marine aquatic ecotoxicity potential (MAETP)

This category refers to the toxic substances' impacts on the marine ecosystems. It considers each substance emitted to the soil, water, and air. The unit For MAETP is kg of 1,4-dichlorobenzene equivalents (1,4-DB eq) per kilograms of emission. Using container ships, several materials are transported from one place to another across the sea; therefore, this impact category is considered.

2.6.4. Acidification potential (AP)

AP refers to the compounds that are precursors to acid rain. These cover nitrogen oxides (NO_X), nitrogen dioxide (N_2O), nitrogen monoxide (NO), sulfur dioxide (SO_2), and several different substances. It could have a vast effect on surface water, ecosystems, soil, groundwater, and materials. This category is expressed by SO_2 equivalent/kilograms emission. As far as the battery system is considered, acidification potential is quite relevant. For

instance, sulfur trioxide (SO_3) utilized in battery manufacturing is a constituent of acid rain.

2.6.5. Human toxicity potential (HTP)

This category refers to the potential harm of a chemical released unit into the environment based on a compound's potential dose and inherent toxicity. It is expressed in kg, 1,4-DCB equivalents. The battery could include toxic materials such as Nickel. For instance, Environmental Protection Agency (EPA) has categorized several nickel compounds as carcinogenic to humans (Toxicological Profile for Nickel, 2005).

3. Results and discussion

3.1. Vanadium redox flow battery system

The battery system in this study is VRF-B. This system's electrolytes are contained within the cell, same as conventional batteries, and there are two independent tanks where the electrolytes are stored. The catholyte (positive electrolyte) and anolyte (negative electrolyte), the tanks fluids (including electrolytes), are pumped into the battery stack. The amount of liquid is always the same as the electrolytes tanks' amount; however, each oxidation state species will rely on the system operation's reaction times. The membranes within this system can separate electrolytes in the cell, avoiding mixing with the redox species. Concurrently, it enables the ions transfer to maintain the system electroneutrality (GaBi, 2021; Mostert et al., 2018). The energy source for the use phase of this system is PV. According to the installed PV technologies, the PV is modeled by the global average market mix of Multi-silicon 47%, Mono-Silicon 42% Copper-Indium-Gallium-Diselenide 4%, and Cadmium-Telluride (CdTe) 7%. The system has considered the manufacturing and operation stages. The panels' end-of-life stage is excluded due to a lack of standard technologies to recycle or reuse. The panel's operational lifetime is taken as 20 years. Mono-silicon 18%, Cadmium-Telluride (CdTe) 17%, Multi-Silicon 16%, and Copper-Indium-Gallium-Diselenide 15% average efficiencies are utilized per technology. In comparison, a different study (da Silva Lima et al., 2021) has also conducted a LCA for the VRF-B system with the same lifetime of 20 years, with electricity from a renewable source for operating the system.

The outcomes of the LCA analysis reveals that the overall GWP impact for the VRF-B system is 0.121 kg CO_2 eq./kWh. Fig. 5(a) shows the contributors to the global warming potential (GWP) for the redox flow battery system components. Three components mainly responsible for the GWP are container ship, district heating, and PV electricity. The highest component contributing to the GWP impact in this system comes from the electricity production from PV, with a percentage of 68%. It corresponds to 0.0743 kg CO_2 eq./kWh, whereas the container ship is 5% with a value of 0.00536 kg CO_2 eq./kWh. The PV is used as the energy input for the use stage of the battery. Although PV uses a renewable energy source as an input with zero impact on electricity generation, the system's manufacturing itself is harming the environment. There are hazardous materials included in the manufacturing process of PV cells as they are utilized to purify the semiconductor's surface. These chemicals include nitric acid, 1,1,1, -trichloroethane, and sulfuric acid, etc. For instance, 1,1,1, -trichloroethane is a substance that contributes to the most impact as it is a greenhouse gas that causes the increased greenhouse gas impact. On the other hand, the container ship and the other systems components contribute to 5% and 13%, respectively, of this category's total impact. In the literature (Mostert et al., 2018), heating production accounts for 32% of the GWP, whereas it is 14% in this study. Similarly, Weber et al. (2018) have conducted a LCA of VRF-B, and it was observed that electricity demand accounts for more than 30% of the GWP impact. It was also indicated that the grid electricity is a significant source of the environmental impacts, causing a high contribution in GWP.

The ozone layer depletion potential (ODP) contribution for the VRF-B is presented in Fig. 5(b). The copper and roll-formed metal are the main contributors to the ODP impact for VRF-B. The roll-formed metal represents 97% of the total impact with a value of 4.38×10^{-10} kg R11 eq./kWh. Steel production causes severe environmental impacts, including carbon monoxide as air emissions that can affect the stratospheric ozone layer. On the other hand, copper has only a 3% impact on this category with a value of 1.26×10^{-11}kg R11 eq./kWh. Gouveia et al. (2020) have conducted a LCA for VRF-B of the same lifetime and functional unit, excluding the use and waste of the system. Due to their high volume, the transportation of the materials has accounted for most of the impacts. Except for the ODP category, the contribution was negligible. It was observed that increasing the battery's storage capacity from 1 kWh to 180 kWh led to a reduction of 90% in ODP (Weber et al., 2018).

Fig. 5(c) shows that the human toxicity potential (HTP) of VRF-B. HTP category is very significant for batteries since many toxic chemicals are employed during manufacturing. For this study, the copper sheet mix used to manufacture batteries accounts for most of the impact. It represents almost 100% of the total impact, equivalent to 2.34 kg DCB eq./kWh. Long-term exposure to copper results in nose, eyes, or mouth irritation; therefore, it could cause dizziness, headaches, stomachaches, etc. At least 20% loss of olfactory sensation function is caused by copper's slightest concentration (Solomon, 2009). In comparison, the other materials represent only 0.00155 kg DCB eq./kWh showing negligible impact.

In Fig. 6(a), the MAETP impact is mainly caused by steel hot rolled, copper sheet, and PV electricity. The copper component involved in the manufacturing stage is the main impact contributor for MAETP. It accounts for more than half of the impact representing 65% (52.9 kg DCB eq./kWh) of the total impact contribution in the MAETP category as depicted in Fig. 6(a). Copper metal is one of the most toxic to ecosystems and aquatic organisms. Therefore, once fish is exposed to copper concentrations, they lose their sense of smell, which lessens their appetites. Aquatic animals are more sensitive to the metal's toxic effects than aquatic plants (Solomon, 2009). In the MAETP category, the hot rolling steel shows only 3% contribution with a value of 2.21 kg DCB eq./kWh.

In Fig. 6(b), the AP impact is distributed among sulfur trioxide, PV electricity, and container ship. It is indicated that the PV is a significant contributor to AP impact. It shows 55% of the total contribution corresponding to 0.000273 kg SO_2 eq./kWh as the PV system requires some chemicals/substances such as nitric acid. Acid rain is caused by nitrogen oxides and sulfur dioxide (NO_X and SO_2); as they are emitted into the air, the air and wind currents transport them. These two chemicals react with oxygen, water, and several chemicals to form nitric acid. In comparison, the sulfur trioxide has the least acidification potential contribution of only 4% with an impact of 0.0000207 kg SO_2 eq./kWh. In the literature (Weber et al., 2018), transportation accounted for more than 38% of the AP impact. The literature included the whole life cycle, whereas this analysis has excluded maintenance, disposal, and recycling phases, explaining the differences in impact distributions.

3.2. Compressed air storage system

An underwater compressed air storage system is considered for this study. The underwater compressed air system can bear various configurations, like those included or utilized for underground CAES (e.g., diabatic/adiabatic, etc.). The main difference

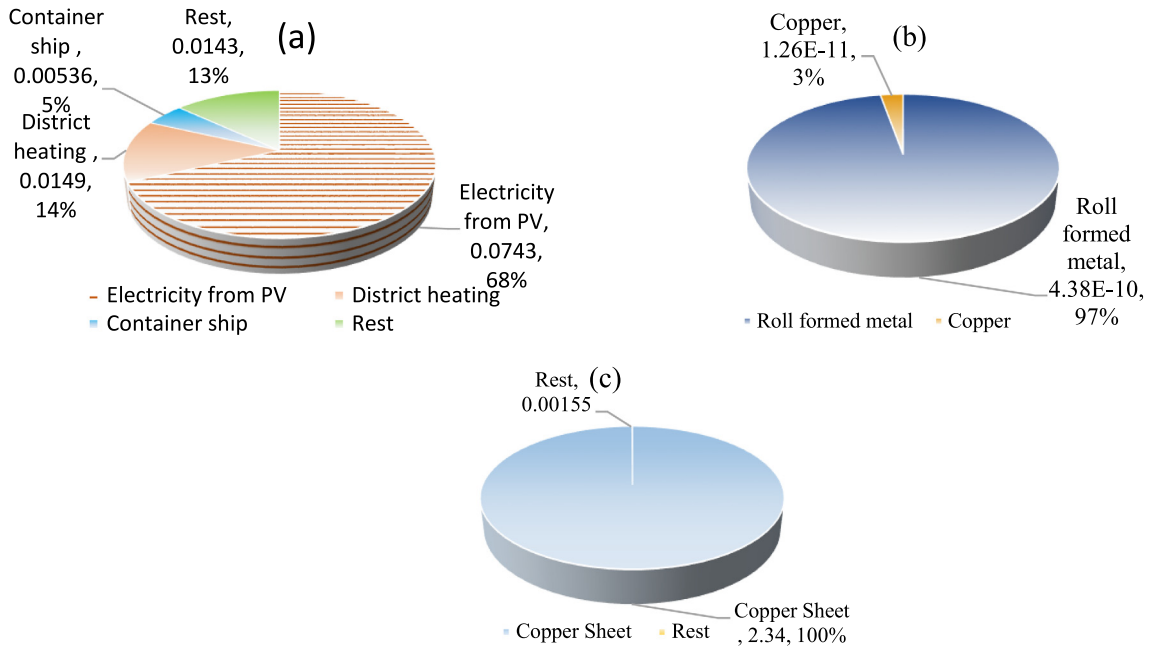

Fig. 5. Impacts contribution of (a) GWP, (b) ODP, and (c) HTP for VRF-B system.

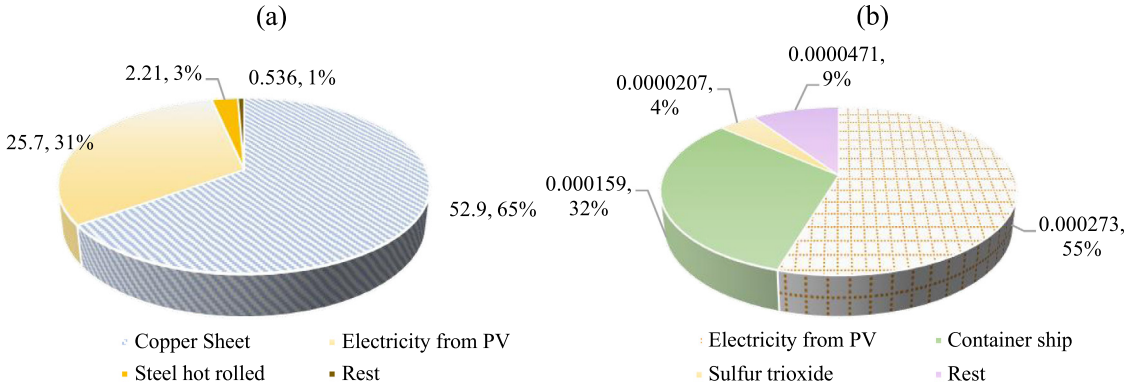

Fig. 6. Impacts contribution of (a) MAETP and (b) AP for VRF-B system.

between the underground CAES and underwater CAES is the characteristic of the pressure. This difference assists in enhancing the underwater system's roundtrip efficiency over the underground one (Pete et al., 2015). This system compresses air by utilizing electric generators as the air is compressed. When electricity is required, water weight pushes the air to the surface by an airline to an expander, where the air is converted into electricity. The offshore environment offers some ideal conditions for compressed air storage. By pressuring air storage in an underwater vessel, the air/water barrier loading is significantly reduced due to the surrounding water's air pressure. The underwater compressed air system is still under development; it is an attractive method as it is essentially a variant of the pumped hydro system. Typically, for such storage, to produce 1 kWh/m^3, a depth of 99 m is required. The nominal storage capacity and discharge energy amount per day are 2000 and 1070 kWh/m^3 (Mostert et al., 2018; Pete et al., 2015). In this work, the CAES system utilizes PV as the energy source of the use phase, similar to the VRF-B system. The total GWP impact of the CAES is 0.117 kg CO_2 eq./kWh. The total impact is distributed mainly among stainless steel, naphtha, and PV electricity. Another study (Kapila, 2018) has calculated a GWP impact of 0.293 kg CO_2 eq./kWh for a conventional CAES when using solar PV. The literature value varies compared to the obtained values as the disposal and maintenance phases were not covered. In addition, the evaluated CAES system is an underwater type, whereas the literature has considered an underground system. Note that the impact contribution is similar to the VRF-B for the GWP impact. Here, the PV power production process shows the highest GWP impact as it contributes 94% (0.106 kg CO_2 eq./kWh) of the total impact, as shown in Fig. 7(a). As solar PV manufacturing embodies different chemicals, not only 1,1,1-trichloroethane contribute to the GHGs emissions, but acetone is also included. Acetone acts as a greenhouse gas and could influence cloud formation (Arnold et al., 1997). In contrast, stainless steel contributes the least GWP impact among all CAES components as it is only 1% (0.00147 kg CO_2 eq./kWh). In the literature study (Mostert et al., 2018), the use of iron and low-alloy steel contributed to more than half of the global warming impact as it was 52%. In comparison to literature, PV is utilized as a source of energy for the use phase of the system, whereas the literature did not specify the energy type and focused on the storage phase only.

Fig. 7(b) shows that both polyethylene HDPE and PV electricity are the main contributors to ODP impact. The PV process contributes to the most ODP impact of 79% and with a value of 5.62×10^{-13} kg R11 eq./kWh. The PV system production utilizes

chemicals that could potentially harm the ozone layer, e.g., 1,1,1-Trichloroethane, as it is one of the ozone-depleting substances according to environmental guidelines (Alternatives, 2007). On the other hand, High-Density Polyethylene (HDPE) contributes to the least ozone layer depletion impact as it represents only 21% (1.46×10^{-13} kg R11 eq./kWh) of the total effect as shown in Fig. 7(b). The compressed air must be delivered with enough volume, adequate pressure, and quality to precisely power the components that utilize the compressed air. HDPE is utilized for the compressed air piping system, as it does not corrode and minimizes the energy to push compressed air through the compressed air system. Although the waste contribution was not included in this analysis, the impact was shown to be negligible for most of the impacts like ozone depletion, acidification potential, etc, as reported in the literature (Weber et al., 2018).

Fig. 7(c) represents the PV process as the only component responsible for most of the HTP impact (97%), corresponding to 0.0528 kg DCB eq./kWh. For PV cell production, several chemicals, e.g., sulfuric and hydrochloric acid, are utilized to clean the surface of the semiconductor. These chemicals are harmful if inhaled by humans. On the other hand, the rest of the materials (e.g., stainless steel) show only an impact of 0.00161 kg DCB eq./kWh. When stainless steel products are in their solid-state, no ingestion, inhalation, or contact health hazard could occur in terms of HTP (Precision Specialty Metals, 2015).

PV process contributes to most (98%) of the impact for MAETP than the other system components with a value of 36.7 kg DCB eq,/kWh as shown in Fig. 8(a). Leaks of the chemicals utilized to make PV cells could be potentially hazardous to the aquatic life as it is shipped to the construction site. In comparison, the other system components represent only 2% (0.56 kg DCB eq./kWh). In Fig. 8(b), it is shown that the only impact contributors are the PV process and stainless steel.

The electricity coming from the PV contributes to 79% of the CAES's AP impact with a value of 0.000391 kg SO_2 eq./kWh. On the other hand, stainless steel represents less impact of 21% of the total with a value of 0.000102 kg SO_2 q./kWh. It is perceived as highly durable and easily maintained (Rossi, 2012).

3.3. Molten salt thermal energy storage

In this system, heat transfer fluid passes through the solar collector assembly as it gets heated. Then, the thermal energy is directly carried to the steam generator by the heat transfer fluid for electricity production or to the location where obtained thermal energy is exchanged with cold molten salt to increase the temperature. After that, the hot tank storage receives the pumped hot molten salt. A reverse action occurs during cloudy conditions or at night. The heat transfer fluid passes through the heat exchanger, as the stored heat in molten salt is carried to the steam generator for electricity production. To start a new cycle, the cold molten salt is then pumped to the cold tank. The cold tank is equipped with heaters to avoid molten salt freezing maintain temperatures above certain temperature. It was indicated that for molten salt thermal storage, concrete is preferable for thermal storage (Adeoye et al., 2014).

The GWP impacts obtained for different concentrated solar plants (CSP) are less than 40 kg CO_2 eq./MWh (Pelay et al., 2020). The components mainly responsible for the GWP impact are steel sections, land space, and steel tinplate. Utilizing the land space of 0.000415 m^2 per kWh for the solar field construction contributes to the most global warming impact (58%) with a value of 0.0146 kg CO_2 eq/kWh as shown in Fig. 9(a). Industrial processes cause unfavorable environmental effects, resulting in loss of natural resources, air and water, and global warming. On the other hand, steel tinplate represents only 5% (0.00128 kg CO_2 eq./kWh). Steel tinplate is one of the well recyclable materials, as it can return to the production cycle with no quality loss. In the literature (Adeoye et al., 2014), the highest impacts come from fossil fuel needed for power generation; however, for this study, electricity grid mix is used instead of the diesel energy in the molten salt construction phase. By excluding the storage phase, the GWP impact could be reduced by approximately 6% (Pelay et al., 2020).

In Fig. 9(b), the ODP impact of the molten salt system is distributed only among fiberglass and concrete. Fiberglass contributes to 90% of the total contribution in the ODP category corresponding to 2.84×10^{-10} kg R11 eq./kWh as indicated in Fig. 9(b). The fiberglass fabrication process could lead to toxic air pollutant emissions, namely, styrene. It is the major contributor to pollution. Solvents, paints, adhesives, and thinners can release several volatile organic compounds (VOC) and air pollutants. These chemicals can react in the air to create smog (ground-level ozone), related to several respiratory impacts (Environmental Protection Agency, 2005). On the other hand, concrete accounts for 10% of the impact having 3.24×10^{-11} kg R11 eq./kWh.

The three components mainly responsible for the MAETP impact are land space, sodium chloride, and fiberglass, as presented in Fig. 9(c). Fiberglass plastic represents the highest MAETP as it represents 39% of the total impacts and is 0.965 kg DCB eq/kWh, as shown in Fig. 9(c). The most disturbing marine impact is caused by plastic, as it can result in suffocation, entanglement, and ingestion of numerous marine species. In comparison, sodium chloride has the least impact of only 3% (0.0738 kg DCB eq./kWh). Sea salt contains a significant amount of sodium chloride, and both chloride and sodium have critical functions.

Fig. 10(a) has stainless steel, concrete, and fiberglass as the HTP impact contributors of the molten salt system. Stainless steel contributes the most human toxicity potential impact compared to other materials. As shown in Fig. 10(a), 68% of the total impact (0.00312 kg DCB eq./kWh) is due to stainless steel. Nickel and chromium may cause health concerns. For instance, Nickel could have a side effect on humans, such as allergy. In contrast, the concrete used for molten salt storage manufacturing shows the least impact of 6% (0.000296 kg DCB eq./kWh).

Fig. 10(b) represents fiberglass, steel tinplate, and land space as the components responsible for the AP impact. It is shown that the fiberglass plastic has the highest AP as it represents 43% with a value of 0.0000258 kg SO_2 eq./kWh. It is analogous to the ozone layer depletion impact contribution as the fiberglass represents the most impact and releases toxic air pollutants. In comparison, the steel tinplate is shown to have the least impact of only 2% (0.00000323 kg SO_2 eq./kWh). It was found that including on-site water and material recycling could reduce the molten salt storage system overall impacts and implement a different material to the molten salt, e.g., concrete (Adeoye et al., 2014).

3.4. Overall environmental comparison

The three energy storage systems' are presented in Fig. 11(a). It is indicated that the VRF-B has the highest impact of 0.121 kg CO_2 eq./kWh, whereas the CAES comes second with a value of 0.117 kg CO_2 eq./kWh and last is the molten salt thermal storage as it represents 0.0306 kg CO_2 eq./kWh. The compressed air system has the PV process as the primary contributor for this impact category as it is a significant contribution to the GHGs emissions, including acetone and 1,1,1-trichloroethane. Similarly, battery storage utilizes electricity from PV as an input for the system use stage.

In comparison, the electricity of PV for the CAES represents 0.106 kg CO_2 eq./kWh. At the same time, the PV utilized for the VRF-B contributes to 0.0743 kg CO_2 eq./kWh of the total

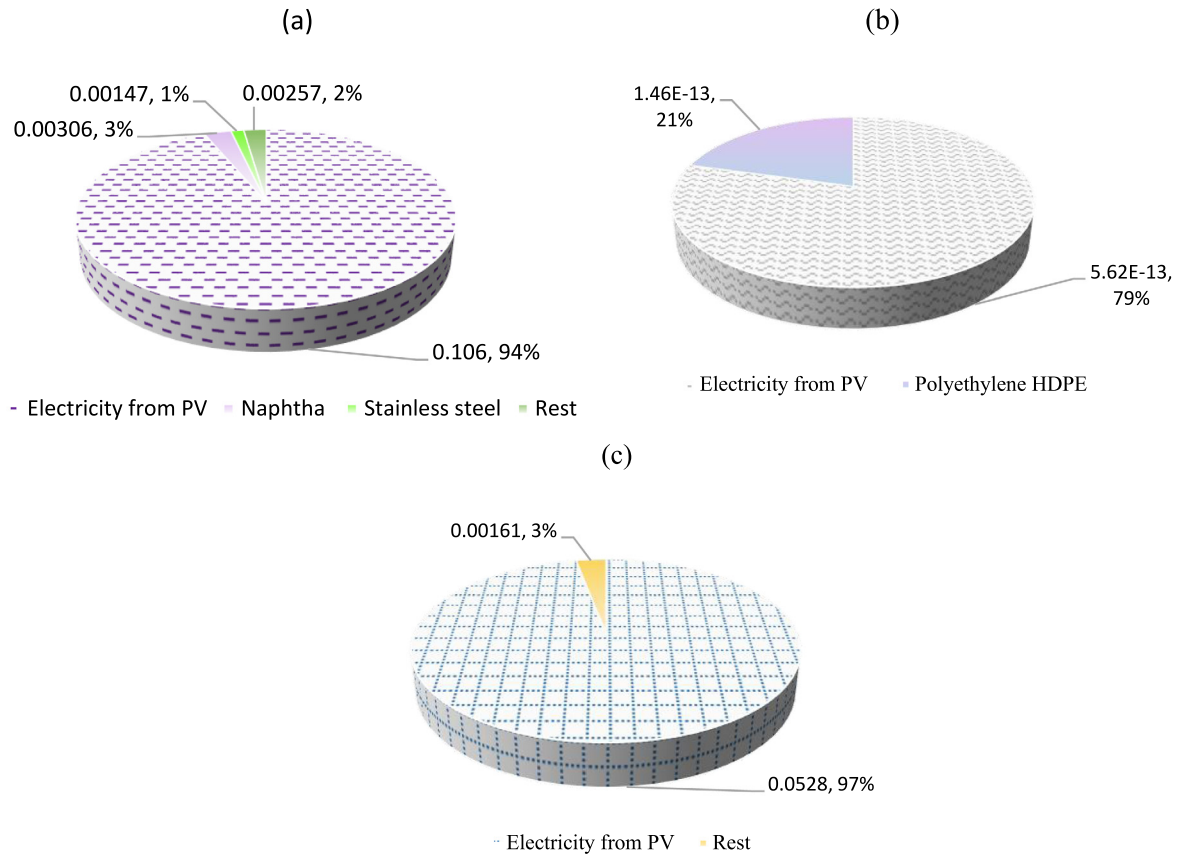

Fig. 7. Impacts contribution of (a) GWP, (b) ODP, and (c) HTP for CAES system.

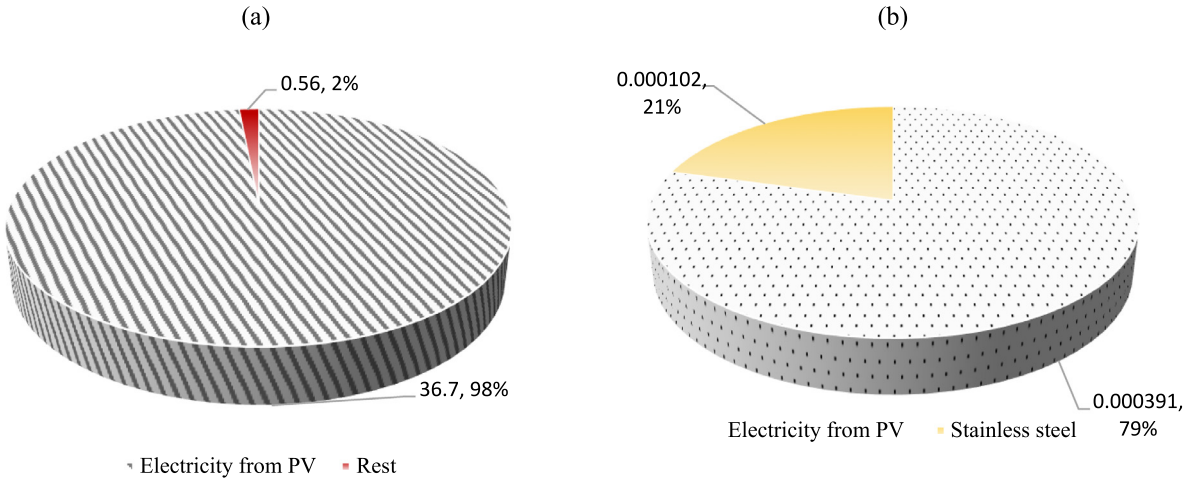

Fig. 8. Impacts contribution of (a) MAETP and (b) AP for CAES system.

impact, including the heating district of 0.0149 kg CO_2 eq./kWh. On the other hand, the solar field's construction stage has the most materials utilization for the molten salt as the steel sections are mainly used for the system. The steel section represents 17% of the total impact for this category and is the primary material leading to global warming for the molten salt system. This system utilizes the electricity grid mix for the system use stage.

Fig. 11(b) represents the overall ODP impact for all systems. The highest impact among the three is the VRF-B (2.87×10^{-10} kg R11 eq./kWh). The molten salt system is 1.12×10^{-10} kg R11 eq./kWh and the lowest ODP impact is for the CAES as it is 7.24×10^{-13} kg R11 eq./kWh. For the molten salt, fiberglass represents most of the impact (90%) in the ODP category. As far as fiberglass fabrication production is concerned, emissions of toxic air pollutants are emitted. The fiberglass fabrication process of the solar field construction, e.g., paints or solvents, could release some hazardous air pollutants or volatile organic compounds. The chemicals of these substances could react in the air, making the ground-level ozone (smog). Compared to the molten salt and VRF-B, the CAES has a very slight and non-visible impact, as shown in Fig. 11(b), and is only 2.07×10^{-12}kg R11 eq./kWh. The CAES's main contributor to this impact is the PV process, representing 79% of this category's total impact.

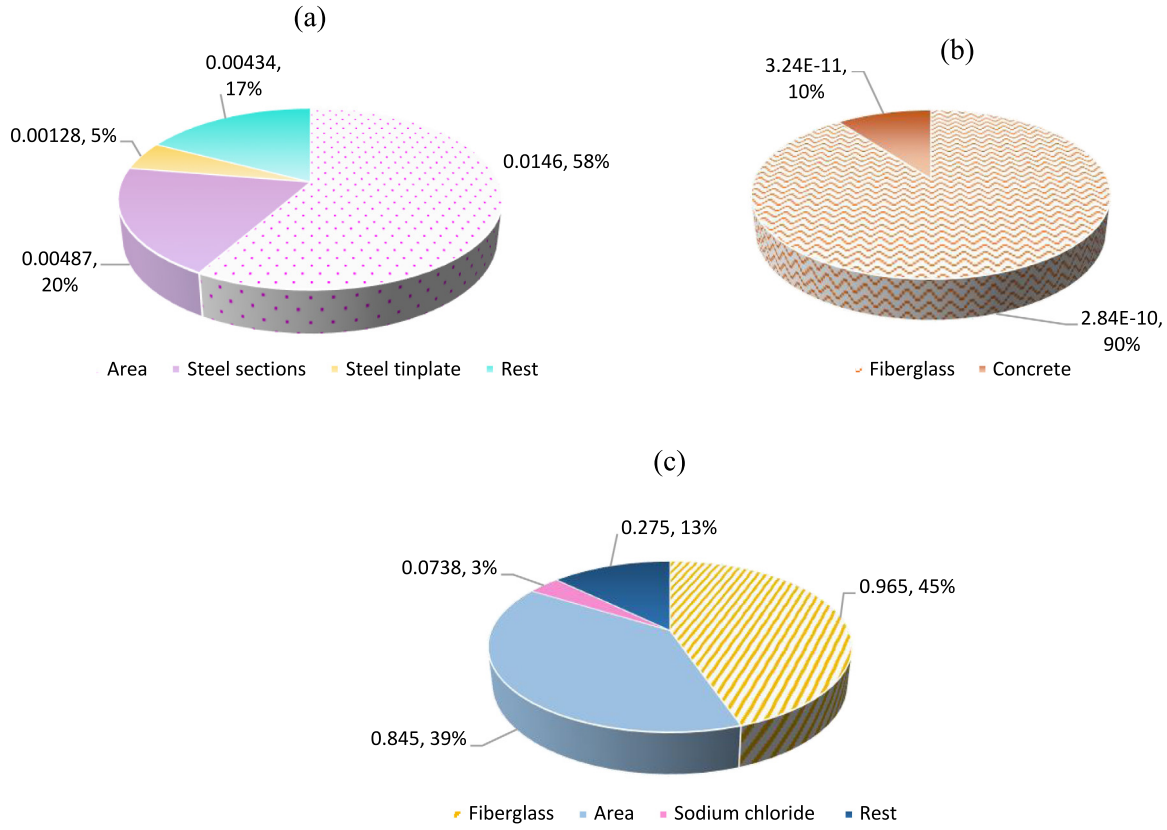

Fig. 9. Impacts contribution of (a) GWP, (b) ODP, and (c) MAETP for molten salt system.

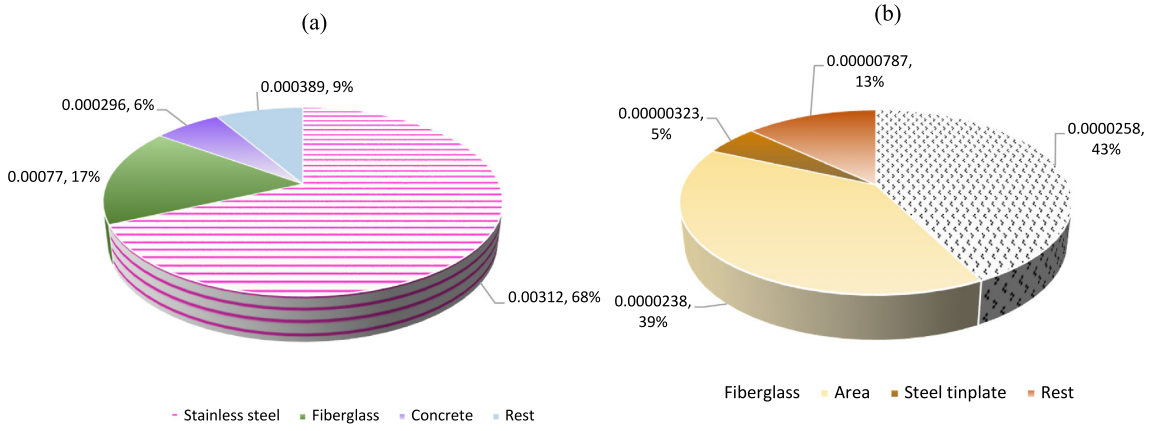

Fig. 10. Impacts contribution of (a) HTP and (b) AP for the molten salt system.

The HTP impacts for all methods are shown in Fig. 12(a); the VRF-B leads to the most HTP impact of 2.38 kg R11 eq./kWh. Copper is the significant impact contributor for this category as it shows 100% of the total impact. The HTP for the VRF-B is commonly associated with, e.g., Nickel, Cobalt, Copper, etc. The CAES has copper as the second leading contributor after the PV process. The molten salt system has an insignificant impact and is barely visible in Fig. 12(a), with a value of 0.0058 kg R11 eq./kWh. The molten salt has stainless steel as the primary contributor; however, it is not a major concern when for instance, compared to the impact of copper, as it represents 100% of the total impact for VRF-B.

Fig. 12(b) shows that the VRF-B has the highest AP impact, representing 0.000545 kg SO_2 eq./kWh. PV contributes to more than half of the impact than the other system components as it is 55%. The CAES system is similar as PV has the highest impact of 79%. In contrast, the molten salt system has the most negligible AP impact of 0.0000786 kg SO_2 eq, with fiberglass showing the most AP impact, as it releases toxic air pollutants.

The VRF-B impact for the MAETP is significantly high compared to both molten salt and CAES systems impacts with a value of 85.1 kg DCB eq./kWh as shown in Fig. 12(c). The CAES comes after the VRF-B with 40 kg DCB eq./kWh. Copper is the leading material for this category, with 65% of the total impact. The copper impact of VRF-B itself contributes to 52.9 kg DCB eq./kWh. On the other hand, the plastics used for the molten salt system show 45% of the impact, leading to numerous marine species issues.

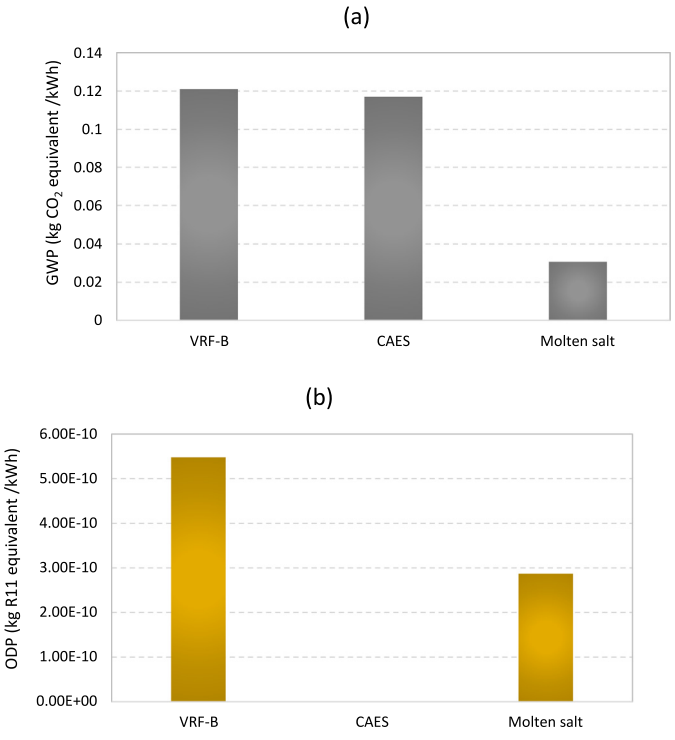

Fig. 11. Overall impacts comparison of (a) GWP and (b) ODP for the storage systems.

3.5. Sensitivity analysis

A sensitivity analysis was conducted to investigate the effects of changing the main contributing processes having the highest impacts with other alternatives. In this way, it is investigated whether there will be an improvement in the overall emissions. The processes replaced for VRF-B, CAES, and molten salt systems are copper, energy source, and steel type. For the CAES, electricity from the PV is the main reason for the high impacts of different CAES system categories. Therefore, electricity from the grid mix is utilized to replace PV to present how the new scenario's results differentiate from the base case. In comparison, the overall GWP impact is reduced by 85% when using renewable energy source (PV) instead of electricity grid mix, as shown in Fig. 13(a). The PV electricity generation does not emit any greenhouse emissions; it is only the construction stage for the PV system responsible for the indicated GWP impact.

Several equipment utilized in the transmission and distribution system for the electricity grid are insulated with sulfur hexafluoride. The ODP impact is higher by 74% for the PV than the electricity grid source, as shown in Fig. 13(b). On the other hand, the MAETP impact is 30% less for the PV than the electricity grid in Fig. 13(e), representing 39.9 kg DCB eq./kWh. Whereas in Fig. 13(c), the HTP impact is slightly close for both as it is 0.101 and 0.079 kg R11 eq./kWh and is 21% less when using grid electricity. The same is valid for the VRF-B scenarios comparison in Fig. 14; using grid mix electricity has significantly increased the overall GWP impact by 17.2%. It becomes about 0.541 kg CO_2 eq./kWh as given in Fig. 14(a). Except for the ODP and HTP impact in Fig. 14(b) and (c), the ODP impact remained the same with 5.48×10^{-10} kg R11 eq./kWh, while the HTP impact has only increased by 0.42% for the PV source.

In the VRF-B system, a copper sheet is replaced with an aluminum sheet as most of the impacts are caused by copper.

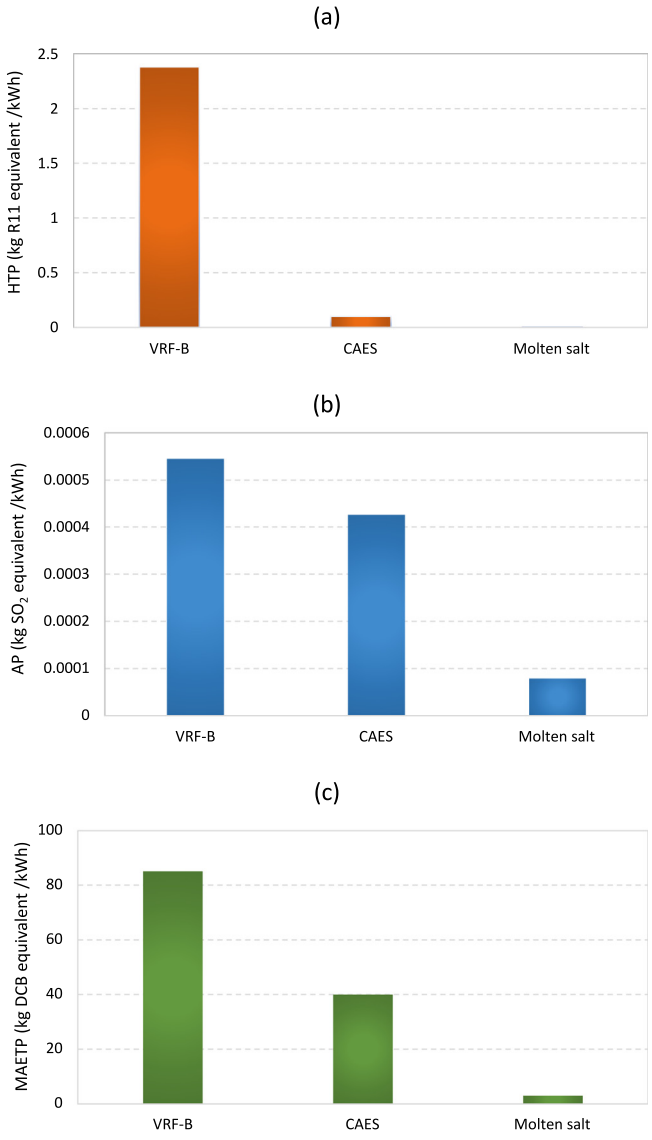

Fig. 12. Overall impacts comparison of (a) HTP, (b) AP, and (c) MAETP for the storage systems.

Aluminum is used as it is a common alternative to copper. Fig. 15 represents the overall impacts for the battery system when utilizing either copper or aluminum sheets. The GWP impact in Fig. 15(a) remained the same for both scenarios, representing 0.121 kg CO_2 eq./kWh. In Fig. 15(c), the HTP impact of aluminum is significantly lower by 95.8% than copper as it shows 0.0402 kg R11 eq./kWh. Exposure to aluminum is generally not harmful. However, exposure to high concentrations is not favorable either. In comparison, the MAETP impact in Fig. 15(e), the copper impact is significantly higher than aluminum by 63.4% approximately. Aquatic animals are sensitive to the metal's toxicity; copper and aluminum are toxic materials to the aquatic environment, regardless of these materials' concentration exposure level (Solomon, 2009).

The type of steel is changed from regular steel to stainless steel for the molten salt system's solar field manufacturing stage. Fig. 16 represents the two steel types and how they impact the overall results. Both sheets of steel differentiate in their properties, whether for ductility, hardness, or strength. The stainless-steel impact for GWP impact is slightly higher by 16.3% than regular steel, as shown in Fig. 16(a). Stainless steel requires more

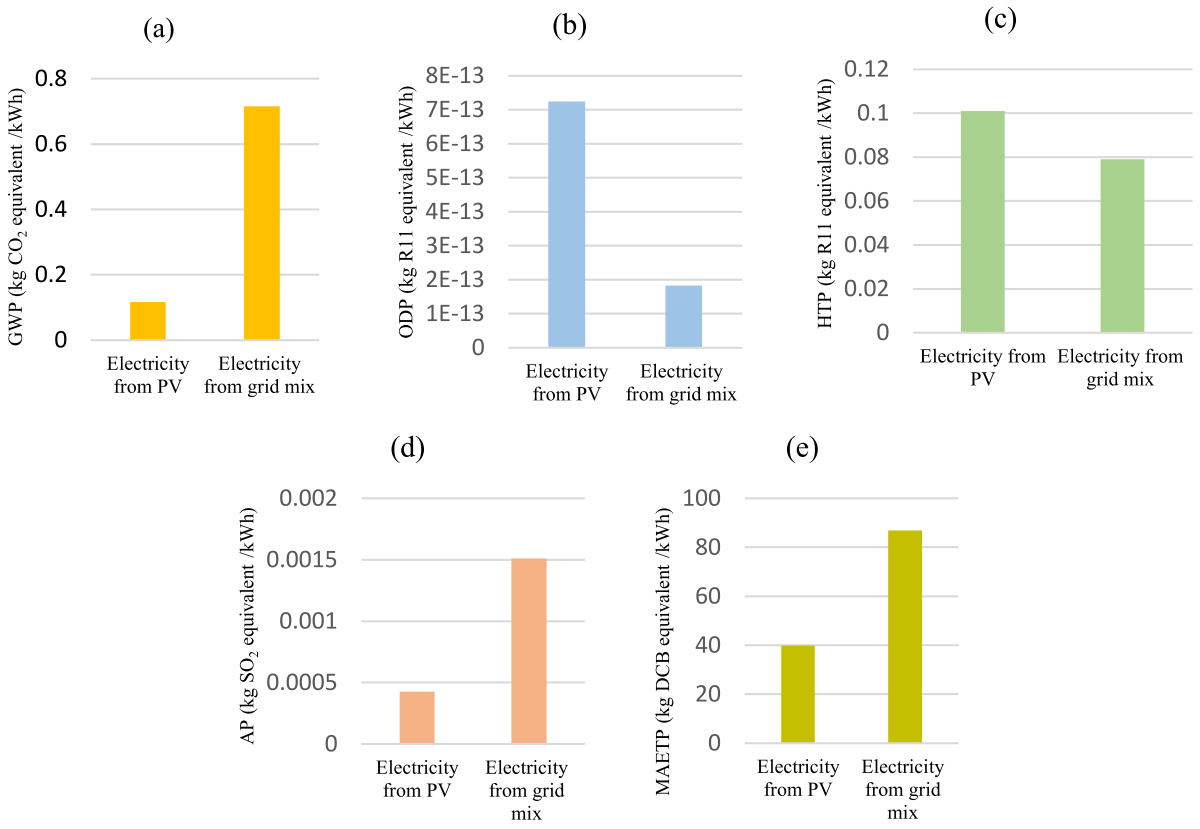

Fig. 13. Overall CAES impacts: (a) GWP, (b) ODP, (c) HTP, (d) AP, and (e) MAETP when using either PV or grid mix electricity.

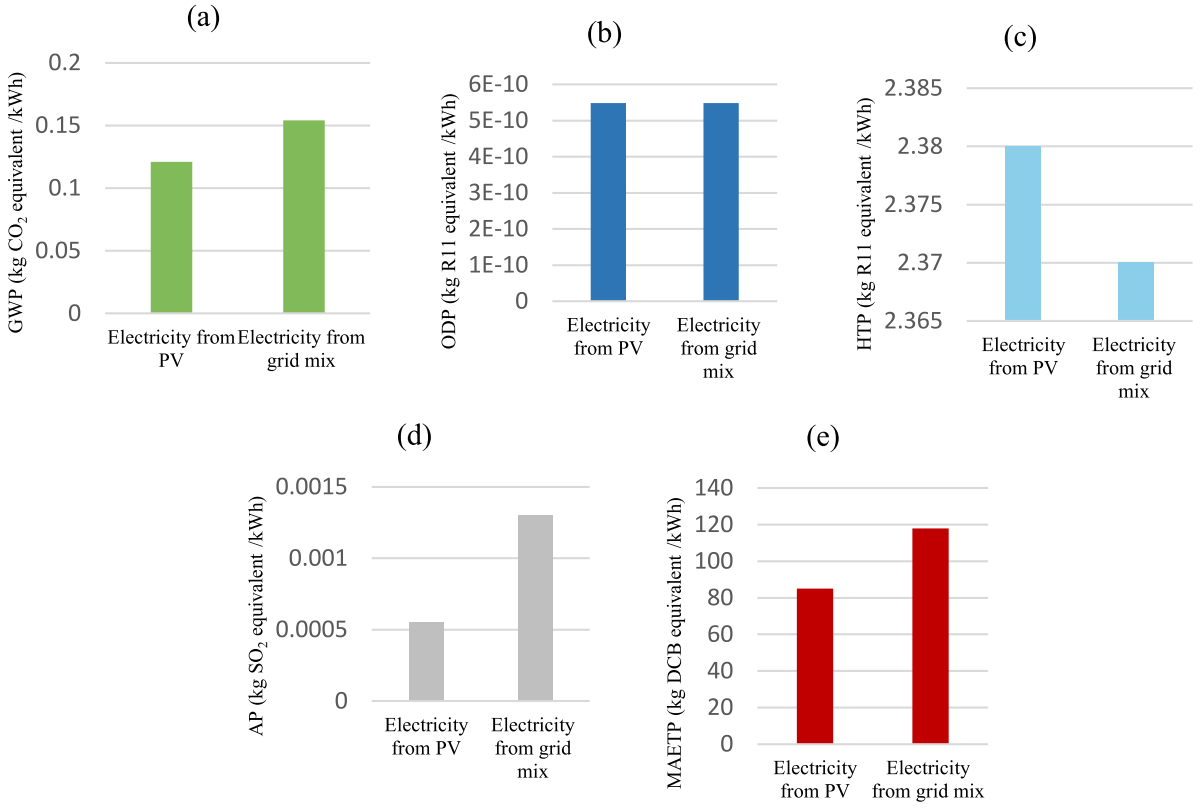

Fig. 14. Overall VRF-B impact: (a) GWP, (b) ODP, (c) HTP, (d) AP, and (e) MAETP when using either PV or grid mix electricity.

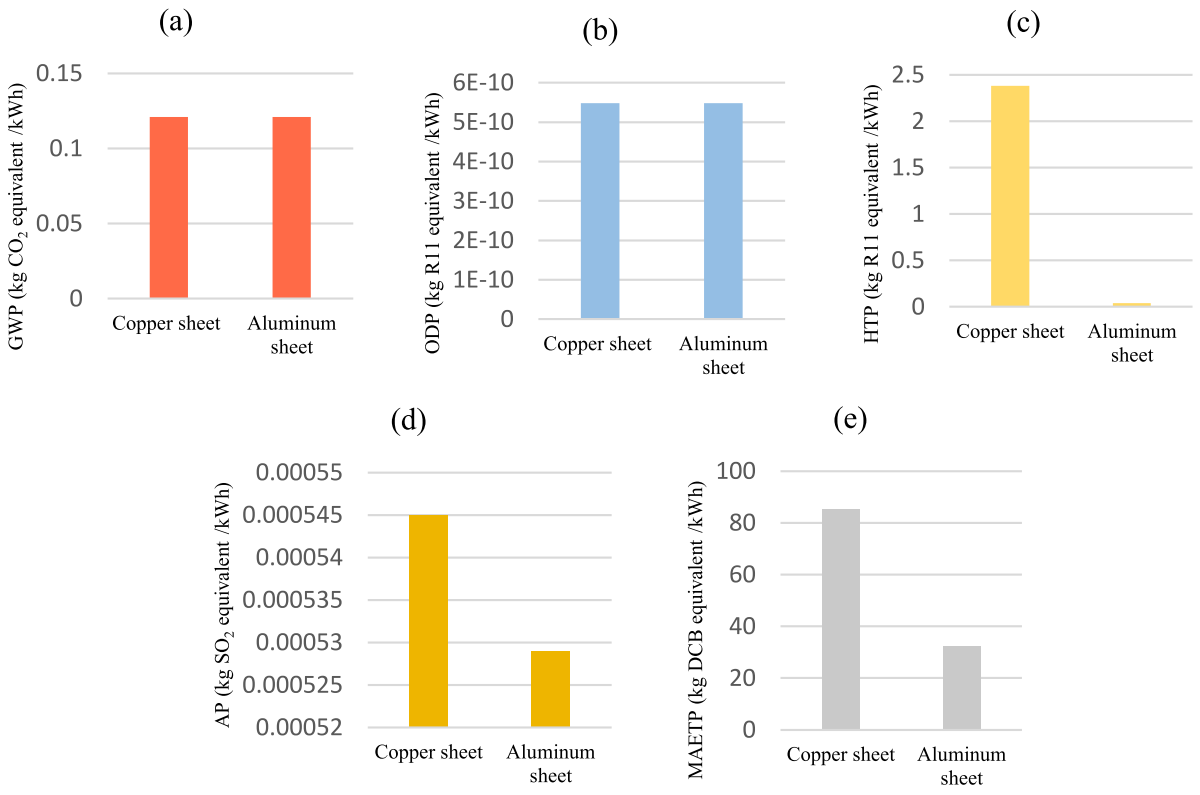

Fig. 15. Overall VRF-B impact: (a) GWP, (b) ODP, (c) HTP, (d) AP, and (e) MAETP when using either Copper or aluminum sheets.

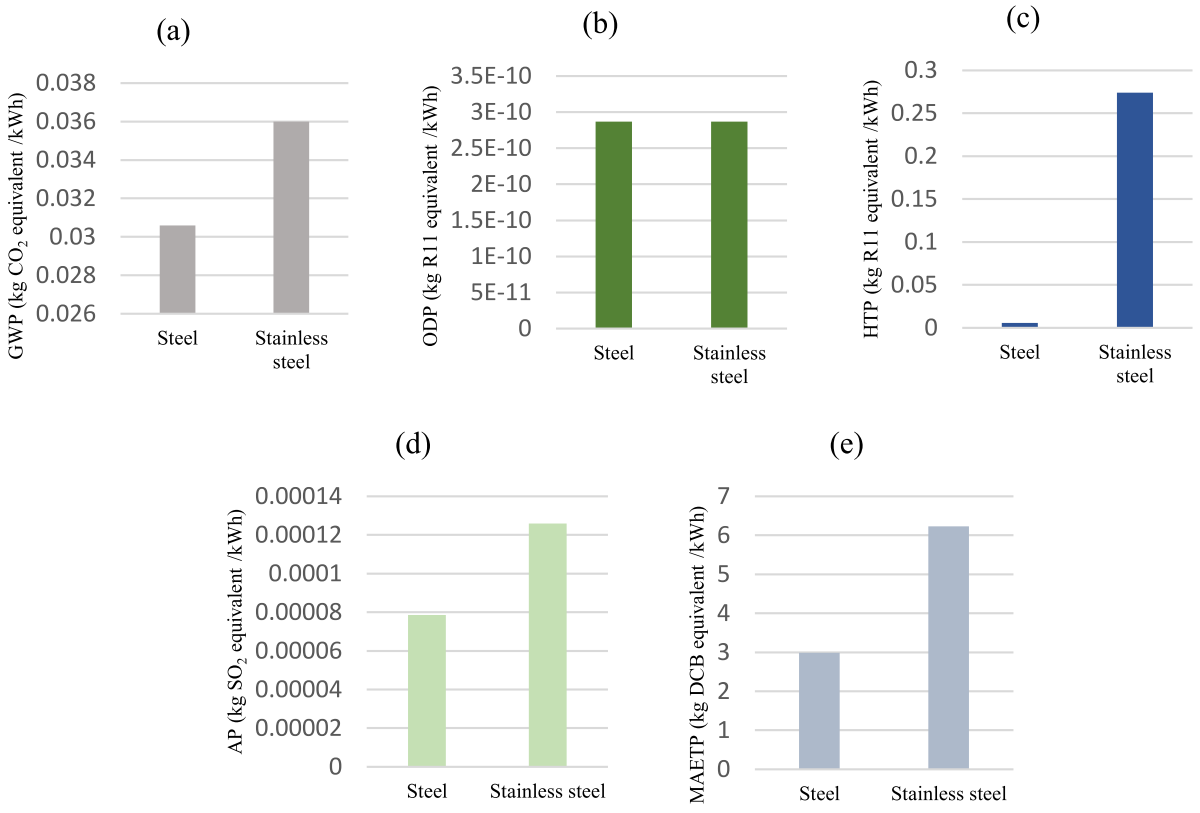

Fig. 16. Overall molten salt system impact: (a) GWP, (b) ODP, (c) HTP, (d) AP, and (e) MAETP when using either steel or stainless steel.

materials for its production compared to regular steel. Besides, the industries that produce stainless steel are energy-intensive industries. Therefore, it is believed to be one of the leading causes of GHGs (Jing et al., 2019). Regular steel has fewer HTP, AP, and MAETP impacts by 34.7–96.3% compared to stainless steel, as shown in Fig. 16(c), (d), and (e). Although stainless steel is more corrosion resistant than other metals, it can still corrode under some circumstances. According to stainless steel's Safety Data Sheet (SDS), the health concern is the dust fumes inhalation that generates due to specific manufacturing procedures, e.g., melting, burning, brazing, etc. (Precision Specialty Metals, 2015).

4. Conclusions

This study conducted a life cycle assessment study to evaluate and compare the CAES, VRF-B, and molten salt energy storage systems to address environmental sustainability. The main motivation of the study is driven by closing the gap between wide implementation of renewable energy resources and limited application of energy storage techniques while addressing the Sustainable Development Goal (SDG) 7 and 13 using a life cycle assessment methodology. Due to their energy density and temperature degradation performances, one method is selected from each main storage classification (electrochemical, thermal, and mechanical). The selected functional unit is one kWh of electricity in which energy production and storage are both accounted for. To have a comprehensive environmental evaluation, diverse impact categories are considered, namely, (i) global warming potential, (ii) ozone depletion potential, (iii) acidification potential, (iv) human toxicity potential, and (v) marine aquatic ecotoxicity potential.

The VRF-B system has shown to be the least environmentally friendly as the impacts are significantly higher than the CAES and molten salt thermal storage systems for all impact categories. The highest GWP impact is obtained for VRF-B corresponding to 0.121 kg CO_2 eq./kWh whereas the least GWP is obtained for the molten salt with a value of 0.0306 kg CO_2 eq./kWh. The VRF-B has the highest ODP impact of 2.87×10^{-10} kg R11 eq./kWh, whereas the CAES has the least. Substances such as cobalt and copper used in the manufacturing of VRF-B cause significant HTP impacts. Similarly, the PV manufacturing phase that is used under VRF-B and CAES has also considerable impacts on both MAETP and HTP.

A sensitivity analysis is conducted to observe the effects of changing several key processes. Using the electricity grid mix as an energy input for the use stage has increased the GWP impact by 0.033 and 0.599 kg CO_2 eq./kWh for the VRF-B and CAES systems, respectively. Compared to the other two methods, the molten salt system has shown the most negligible AP impact of 7.87×10^{-5} kg SO_2 eq./kWh.

The production stage for the systems accounts for the highest share of carbon footprint. As recycling is not included in this study, it could have reduced the systems' material footprint if implemented. Further studies could analyze different energy and materials scenarios to understand better these storage systems' strengths and weaknesses and their possible contribution to the consumption of sustainable materials.

Nomenclature

AP	Acidification Potential
CAES	Compressed Air Energy Storage
CCS	Carbon Capture Storage
CCUS	Capture, Use and Geological Storage
CIS	Copper Indium Selenium
CSP	Concentrated Solar Plant
EPA	Environmental Protection Agency
ESS	Energy Storage Systems
GHG	Greenhouse Gas
GWP	Global Warming Potential
HTP	Human Toxicity Potential
LCA	Life Cycle Assessment
LCIA	Life Cycle Impact Assessment
MAETP	Marine Aquatic Eco-Toxicity Potential
ODP	Ozone Depletion Potential
ORC	Organic Rankine Cycle
TES	Thermal Energy Storage
VRFB	Vanadium Redox Flow Battery

CRediT authorship contribution statement

Manal AlShafi: Formal analysis, Writing – original draft, Investigation, Software, Validation. **Yusuf Bicer:** Conceptualization, Methodology, Software, Supervision, Writing – review & editing, Resources.

Declaration of competing interest

The authors declare that they have no known competing financial interests or personal relationships that could have appeared to influence the work reported in this paper.

Acknowledgment

The authors acknowledge the support provided by the Hamad Bin Khalifa University, Qatar Foundation, Qatar (210028127). Open Access funding is provided by Qatar National Library (QNL).

Appendix A. Supplementary data

Supplementary material related to this article can be found online at https://doi.org/10.1016/j.egyr.2021.09.161.

References

Adeoye, J.T., Amha, Y.M., Poghosyan, V.H., Torchyan, K., Arafat, H.A., 2014. Comparative LCA of two thermal energy storage systems for Shams1 concentrated solar power plant: Molten Salt vs. Concrete. J. Clean Energy Technol. 274–281. http://dx.doi.org/10.7763/jocet.2014.v2.139.

Ahmadi, G., Toghraie, D., Akbari, O.A., 2017. Efficiency improvement of a steam power plant through solar repowering. Int. J. Exergy 22 (2), 158–182. http://dx.doi.org/10.1504/IJEX.2017.083015.

Alqub, A.M., 2017. Design and Life Cycle Assessment of Pumped Hydro Energy Storage System for Nablus Western Wastewater Treatment Plant (Master's thesis). An-Najah National University, Nablus, Palestine.

AlShafi, M., Bicer, Y., 2020. Assessment of various energy storage methods for implementation in hot and arid climates. Energy Storage 2 (6), http://dx.doi.org/10.1002/est2.191.

AlShafi, M., Bicer, Y., 2021. Thermodynamic performance comparison of various energy storage systems from source-to-electricity for renewable energy resources. Energy 219, http://dx.doi.org/10.1016/j.energy.2020.119626.

Alternatives, H., 2007. Environmental guideline for ozone depleting substances (ODS's) and halocarbon alternatives.

Arnold, F., et al., 1997. Acetone in the upper troposphere and lower stratosphere: Impact on trace gases and aerosols. Geophys. Res. Lett. 24 (23), 3017–3020. http://dx.doi.org/10.1029/97GL02974.

da Silva Lima, L., et al., 2021. Life cycle assessment of lithium-ion batteries and vanadium redox flow batteries-based renewable energy storage systems. Sustain. Energy Technol. Assess. 46, http://dx.doi.org/10.1016/j.seta.2021.101286.

Dabiri, S., Khodabandeh, E., Poorfar, A.K., Mashayekhi, R., Toghraie, D., Abadian Zade, S.A., 2018. Parametric investigation of thermal characteristic in trapezoidal cavity receiver for a linear fresnel solar collector concentrator. Energy 153, 17–26. http://dx.doi.org/10.1016/j.energy.2018.04.025.

De Falco, M., Capocelli, M., Losito, G., Piemonte, V., 2017. LCA perspective to assess the environmental impact of a novel PCM-based cold storage unit for the civil air conditioning. J. Clean. Prod. 165, 697–704. http://dx.doi.org/10.1016/j.jclepro.2017.07.153.

Dibazar, S.Y., Salehi, G., Davarpanah, A., 2020. Comparison of exergy and advanced exergy analysis in three different organic rankine cycles. Processes 8 (5), http://dx.doi.org/10.3390/PR8050586.

Environmental Protection Agency, U, 2005. Reducing air pollution from: Fiberglass fabrication operations could your family be affected? [Online]. Available: www.epa.gov/ttn/atw/foam/foampg.html.

Esfandi, S., et al., 2020. Energy, exergy, economic, and exergoenvironmental analyses of a novel hybrid system to produce electricity, cooling, and syngas. Energies 13 (23), http://dx.doi.org/10.3390/en13236453.

Evangelisti, S., Lettieri, P., Borello, D., Clift, R., 2014. Life cycle assessment of energy from waste via anaerobic digestion: A UK case study. Waste Manage. 34 (1), 226–237. http://dx.doi.org/10.1016/j.wasman.2013.09.013.

GaBi, 2021. Life Cycle Assessment. (n.d.). Available: http://www.gabi-software.com/international/solutions/life-cycle-assessment/. Accessed 11 September 2021.

Goedkoop, M., 2013. A Life Cycle Impact Assessment Method Which Comprises Harmonised Category Indicators at the Midpoint and the Endpoint Level, first ed. Ministerie van Volkshuisvesting Ruimtelijke Ordening en Milieubeheer (version 1.08).

Gouveia, J., Mendes, A., Monteiro, R., Mata, T.M., Caetano, N.S., Martins, A.A., 2020. Life cycle assessment of a vanadium flow battery: A joint organization of University of Aveiro (UA), School of Engineering of the Polytechnic of Porto (ISEP) and SCIence and Engineering Institute (SCIEI). Energy Rep. 6, 95–101. http://dx.doi.org/10.1016/j.egyr.2019.08.025, [Online].

Jing, R., Yasir, M.W., Qian, J., Zhang, Z., 2019. Assessments of greenhouse gas (GHG) emissions from stainless steel production in China using two evaluation approaches. Environ. Prog. Sustain. Energy 38 (1), 47–55. http://dx.doi.org/10.1002/ep.13125.

Kapila, S., 2018. Techno-Economic and Life Cycle Assessment of Large Energy Storage Systems (Master's thesis). University of Alberta, Alberta, Canada (unpublished).

Kapila, S., Oni, A.O., Gemechu, E.D., Kumar, A., 2019. Development of net energy ratios and life cycle greenhouse gas emissions of large-scale mechanical energy storage systems. Energy 170, 592–603. http://dx.doi.org/10.1016/j.energy.2018.12.183.

Lacy, R., et al., 2015. Life-cycle GHG assessment of carbon capture, use and geological storage (CCUS) for linked primary energy and electricity production. Int. J. Greenh. Gas Control 42, 165–174. http://dx.doi.org/10.1016/j.ijggc.2015.07.017.

Mostert, C., Ostrander, B., Bringezu, S., Kneiske, T.M., 2018. Comparing electrical energy storage technologies regarding their material and carbon footprint. Energies 11 (12), http://dx.doi.org/10.3390/en11123386.

Oró, E., Gil, A., de Gracia, A., Boer, D., Cabeza, L.F., 2012. Comparative life cycle assessment of thermal energy storage systems for solar power plants. Renew. Energy 44, 166–173. http://dx.doi.org/10.1016/j.renene.2012.01.008.

Pelay, U., Azzaro-Pantel, C., Fan, Y., Luo, L., 2020. Life cycle assessment of thermochemical energy storage integration concepts for a concentrating solar power plant. Environ. Prog. Sustain. Energy 39 (4), http://dx.doi.org/10.1002/ep.13388.

Peng, J., Lu, L., Yang, H., 2013. Review on life cycle assessment of energy payback and greenhouse gas emission of solar photovoltaic systems. Renew. Sustain. Energy Rev. 19, 255–274. http://dx.doi.org/10.1016/j.rser.2012.11.035.

Pete, C., McGowan, J.G., Jaslanek, W., 2015. Evaluating the underwater compressed air energy storage potential in the gulf of maine. Wind Eng. 39 (2), 141–148.

Precision Specialty Metals, I., 2015. Stainless steel safety data sheet (SDS). [Online]. Available: http://www.brownmetals.com/kb/documents/SDS_PSM_Stainless.pdf.

Raugei, M., Leccisi, E., Fthenakis, V.M., 2020. What are the energy and environmental impacts of adding battery storage to photovoltaics? A generalized life cycle assessment. Energy Technol. http://dx.doi.org/10.1002/ente.201901146.

Rehl, T., Lansche, J., Müller, J., 2012. Life cycle assessment of energy generation from biogas - attributional vs consequential approach. Renew. Sustain. Energy Rev. 16 (6), 3766–3775. http://dx.doi.org/10.1016/j.rser.2012.02.072.

Rossi, B., 2012. Stainless steel in structures in view of sustainability. [Online]. Available: http://www.steel-stainless.org/media/1114/22_brossi.pdf, http://www.steel-stainless.org/Content/Files/papers/22_BRossi.pdf.

Solomon, F., 2009. Impacts of copper on aquatic ecosystems and human health. [Online]. Available: https://yukonwaterboard.ca/registers/quartz/qz08-084/Volumes9-11/5.0/5.2.1.pdf.

Stolz, P., Frischknecht, R., Kessler, T., Züger, Y., 2019. Life cycle assessment of PV-battery systems for a cloakroom and club building in Zurich. Prog. Photovolt., Res. Appl. 27 (11), 926–933. http://dx.doi.org/10.1002/pip.3089.

Stougie, L., et al., 2018. Multi-dimensional life cycle assessment of decentralised energy storage systems. In: ECOS 2018 - Proc. 31st Int. Conf. Effic. Cost, Optim. Simul. Environ. Impact Energy Syst.

Toxicological Profile for Nickel, 2005. U.S. Department of Health and Human Services, Public Health Service Agency for Toxic Substances and Disease Registry, Atlanta. Georgia.

Tschiggerl, K., Sledz, C., Topic, M., 2018. Considering environmental impacts of energy storage technologies: A life cycle assessment of power-to-gas business models. Energy 160, 1091–1100. http://dx.doi.org/10.1016/j.energy.2018.07.105.

Vandepaer, L., Cloutier, J., Amor, B., 2017. Environmental impacts of lithium metal polymer and lithium-ion stationary batteries. Renew. Sustain. Energy Rev. 78, 46–60. http://dx.doi.org/10.1016/j.rser.2017.04.057.

Weber, S., Peters, J.F., Baumann, M., Weil, M., 2018. Life cycle assessment of a vanadium redox flow battery. Environ. Sci. Technol. 52 (18), 10864–10873. http://dx.doi.org/10.1021/acs.est.8b02073.

Zhang, X., Bauer, C., Mutel, C., Volkart, K., 2017. Life Cycle Assessment of Power-to-Gas: Approaches, system variations and their environmental implications. Appl. Energy 190, 326–338. http://dx.doi.org/10.1016/j.apenergy.2016.12.098.